DMD Fast Forward. Published on August 31, 2017 as DOI: 10.1124/dmd.117.076455
This article has not been copyedited and formatted. The final version may differ from this version.

PHYSIOLOGICALLY BASED PHARMACOKINETIC (PBPK) MODEL OF THE CYP2D6 PROBE ATOMOXETINE: EXTRAPOLATION TO SPECIAL POPULATIONS AND DRUG-DRUG INTERACTIONS

Weize Huang, Mariko Nakano, Jennifer Sager, Isabelle Ragueneau-Majlessi, Nina Isoherranen

Department of Pharmaceutics, School of Pharmacy, University of Washington, Seattle, WA, 98195

Running Title:

PBPK model of atomoxetine in different populations

Address Correspondence to:

Nina Isoherranen, Ph.D.

Department of Pharmaceutics, School of Pharmacy, University of Washington, H272 Health Sciences Building, Box 357610, University of Washington, Seattle, WA 98195-7610, USA

Tel.: 206-543-2517; Fax: 206-543-3204

E-mail: ni2@u.washington.edu

The Number of

Text Pages: 21

Tables: 6

Figures: 4

References: 44

The number of words in

Abstract: 248

Introduction: 533

Discussion: 1484

Abbreviations: CYP, Cytochrome P450; CI, Confidence interval; DDI, Drug-drug interaction fraction metabolized**;** DIDB, Drug interaction database; EM, extensive metabolizer; HI, hepatic impairment; PBPK, Physiologically based pharmacokinetic; PK Pharmacokinetics; PM, Poor metabolizer; RI Renal Impairment

DMD Fast Forward. Published on August 31, 2017 as DOI: 10.1124/dmd.117.076455
This article has not been copyedited and formatted. The final version may differ from this version.

Abstract

Physiologically based pharmacokinetic (PBPK) modeling of drug disposition and drug-drug interactions has become a key component of drug development. PBPK modeling has also been considered as an approach to predict drug disposition in special populations. However, whether models developed and validated in healthy populations can be extrapolated to special populations is not well established. The goal of this study was to determine whether a drug specific PBPK model validated using healthy populations could be used to predict drug disposition in specific populations and in organ impairment. A full PBPK model of atomoxetine was developed using a training set of PK data from CYP2D6 genotyped individuals. The model was validated using drug-specific acceptance criteria and a test set of 14 healthy subject PK studies. Population PBPK models were then challenged by simulating the effects of ethnicity, drug-drug interactions, pediatrics and renal and hepatic impairment on atomoxetine PK. Atomoxetine disposition was successfully predicted in 100% of healthy subject studies, 88% of studies in Asians, 79% of drug-drug interaction (DDI) studies, and 100% of pediatric studies. However, atomoxetine AUC was overpredicted by 3-4 fold in end stage renal disease and hepatic impairment. The results show that validated PBPK models can be extrapolated to different ethnicities, DDIs, and pediatrics but not to renal and hepatic impairment patients, likely due to incomplete understanding of the physiological changes in these conditions. These results show that systematic modeling efforts can be used to further refine population models to improve the predictive value in this area.

Introduction

Physiologically-based pharmacokinetic (PBPK) models integrate population specific physiological parameters with drug specific physicochemical and pharmacokinetic information to describe and predict drug disposition in various populations (Jones *et al.*, 2009). PBPK modeling has become widespread in drug development, with different model development and acceptance strategies employed at different stages of drug development (Jones *et al.*, 2015). Due to their mechanistic nature and possibility to integrate population-specific physiological changes, PBPK models may allow prediction of drug disposition in challenging clinical situations such as renal and hepatic impairment patients, pediatric population, and pregnant women prior to clinical studies. The confidence in PBPK based preclinical and clinical PK prediction and in drug-drug interaction (DDI) prediction for drugs mainly cleared by cytochrome P450s (CYP) is high (Jones *et al.*, 2015), and the use of PBPK modeling to predict standard drug disposition has been widely recommended (CHMP, 2005; Rowland *et al.*, 2011; CDER, 2012; Huang and Rowland, 2012; Huang *et al.*, 2013). However, while population models for hepatic and renal impairment and for pediatrics have been incorporated into some of the PBPK simulation platforms (Edginton *et al.*, 2006; Johnson *et al.*, 2006, 2010; Edginton and Willmann, 2008; Rowland Yeo *et al.*, 2011), confidence in PBPK modeling in situations involving ethnic variations, pediatrics, renal and hepatic insufficiency and active transport is low or moderate (Jones *et al.*, 2015; Wagner *et al.*, 2015). Overall, it has been reported that the predictive performance of PBPK models in organ impairment populations still remains to be demonstrated, and additional research is needed on system components in this area (Wagner *et al.*, 2015). Limited experience in other specific populations has been stated to prevent conclusions on the predictive performance of PBPK modeling (Wagner *et al.*, 2015). Critically, systematic studies are lacking to delineate the underlying reasons why PBPK modeling approaches

fail to predict drug disposition in specific clinical scenarios. Commonly, this could be due to poor drug model, inaccurate or incomplete population model or low quality and/or inaccurate clinical data. Distinguishing between these causes is particularly challenging as each drug has its own inherent PK variability, and therefore the commonly used n-fold metric to assess model performance may be too stringent for some drugs and too tolerant for others in evaluating model performance (Abduljalil *et al.*, 2014), regardless of population and drug model quality. The aim of this study was to test whether a drug PBPK model validated for healthy volunteers could be extrapolated to special populations with current knowledge of the system components. A recently proposed, statistically rigorous model acceptance criterion (Abduljalil *et al.*, 2014) was used to evaluate model performance to account for drug specific variability in PK data, and to avoid bias from variable quality of clinical data. A rigorous training- validation-extrapolation workflow (Figure 1) was employed to delineate drug specific and population specific factors affecting model performance. Atomoxetine was used as the model compound as it is an FDA recognized, well characterized, and sensitive CYP2D6 probe substrate. Detailed in vitro data on metabolic pathways of atomoxetine and the inhibition of CYPs by atomoxetine is available (Ring *et al*., 2002; Shen *et al*., 2007; Sauer *et al.*, 2004), as well as extensive in vivo intravenous and oral dosing PK data including absolute bioavailability in CYP2D6 genotyped populations (Sauer *et al.*, 2003; CDER, 2002). In addition, atomoxetine pharmacokinetics has been well characterized in pediatric populations (CDER, 2002; Brown *et al.*, 2016), in several different ethnic groups including Japanese and Chinese populations with different CYP2D6 genotypes (Cui *et al.*, 2007; CDER, 2002), and in hepatic impairment populations and end stage renal disease (CDER, 2002; Chalon *et al.*, 2003). As detailed pharmacokinetic parameters for atomoxetine are available in all of the above populations and in thorough drug-drug interaction studies with atomoxetine as a precipitant

or as an object drug (Todor *et al.*, 2015; CDER, 2002; Sauer *et al.*, 2004), atomoxetine provides an ideal model substrate to evaluate comprehensive model validation from healthy adult populations to various special populations and for analysis of population and drug model performance.

Materials and Methods

Data Sources and Subject Demographics. Human clinical PK data available for atomoxetine was collected from the University of Washington Drug Interaction Database (UW DIDB) (http://www.druginteractioninfo.org), NCBI database (http://www.ncbi.nlm.nih.gov/pubmed) and NDA database (http://www.fda.gov/Drugs/InformationOnDrugs), accessed on Jan 1st 2016. Search keywords included "atomoxetine" in NDA and UW DIDB, and "atomoxetine AND pharmacokinetics" in NCBI database. In total, 88 documents were identified that contained information on atomoxetine. Case reports and studies not reporting PK data were excluded, leaving 10 documents with relevant PK data (Belle *et al.*, 2002; CDER, 2002; Chalon *et al.*, 2003; Sauer *et al.*, 2003, 2004; Cui *et al.*, 2007; Matsui *et al.*, 2012; Choi *et al.*, 2014; Todor *et al.*, 2015; Brown *et al.*, 2016). The majority of the identified human PK data were originally reported in the Strattera NDA submission package and later published (Belle *et al.*, 2002; Chalon *et al.*, 2003; Sauer *et al.*, 2004; Matsui *et al.*, 2012). The trials included in the present analysis, and the subject demographics for each trial are summarized in Supplemental Table 1.

Model acceptance criterion. For assessment of model performance, drug specific model acceptance criteria based on variability in observed human PK data for atomoxetine were calculated using recently published methods (Abduljalil *et al.*, 2014) according to equations 1, 2, and 3.

DMD Fast Forward. Published on August 31, 2017 as DOI: 10.1124/dmd.117.076455
This article has not been copyedited and formatted. The final version may differ from this version.

$$\sigma = \sqrt{\ln\left(\left(\frac{CV\%}{100}\right)^2 + 1\right)} \quad (1)$$

$$A\bar{x} = \exp\left[\ln(\bar{x}) + 4.26\frac{\sigma}{\sqrt{N}}\right] \quad (2)$$

$$B\bar{x} = \exp\left[\ln(\bar{x}) - 4.26\frac{\sigma}{\sqrt{N}}\right] \quad (3)$$

In these equations, the CV% represents the observed mean of coefficient of variation (CV) of AUC or C_{max} from all the identified PK trials, and σ is the calculated variability of a given PK parameter in the population. $\bar{x}$ is the observed mean AUC or C_{max}, and N is the mean number of subjects in the clinical studies. The calculated values of A and B are the upper and lower boundaries for acceptable fold error, respectively. The PK studies used for calculation of A and B for AUC and C_{max} included studies in CYP2D6 extensive metabolizers (EM) and poor metabolizers (PM) as summarized in Supplemental Table 2. The calculated acceptance criterion ranges were 0.56-1.77 fold and 0.74-1.35 fold for AUC in EM and PM population, respectively, and 0.76-1.32 fold and 0.75-1.34 fold for C_{max} in EM and PM population, respectively (Supplemental Table 3). Each simulated PK study was compared to the observed values and the results ranked as "acceptable" or "unacceptable" based on whether the mean simulated value was within the acceptance criteria.

PBPK parameter input and model development. The atomoxetine full PBPK model was developed using both "top-down" and "bottom-up" approaches and Simcyp Population-Based Pharmacokinetic Simulator version 14 (Simcyp Limited, Certara, Sheffield, UK) (Jamei *et al.*, 2009). Physicochemical properties and drug specific in vivo PK characteristics were collected from atomoxetine Product Label (https://www.accessdata.fda.gov/drugsatfda_docs/label/2011/021411s035lbl.pdf) and the NDA submission file (CDER, 2002). The fraction absorbed (F_a) for atomoxetine was estimated as 0.96 based on the recovery of atomoxetine and its metabolites in urine following i.v. and oral dosing in

CYP2D6 PM subjects (Sauer *et al.*, 2003). Blood-to-plasma ratio (B/P) and Q_{gut} (Yang *et al.*, 2007), a hybrid term including both villous blood flow and permeability through enterocyte membrane, were predicted in Simcyp.

The fraction of atomoxetine clearance by CYP2D6 ($f_{m,2D6}$) in CYP2D6 EM population was estimated as 87.6% based on the difference in clearances in EM and PM populations using equation 4 (Ito *et al*., 2005):

$$f_{m,2D6} = 1 - \frac{AUC_{EM} D_{PM}}{D_{EM} AUC_{PM}} \quad (4)$$

The final $f_{m,2D6}$ was calculated as a mean value of $f_{m,2D6}$ values calculated from three pairs of genotyped CYP2D6 EM and PM in vivo PK studies in the NDA as shown in the Supplemental Table 4. The remaining hepatic clearance was attributed to CYP2C19, based on a human in vivo study in genotyped individuals assessing the role of CYP2C19 in atomoxetine metabolism (Choi *et al.*, 2014)

The intrinsic clearances of atomoxetine by CYP2D6 ($CL_{int, CYP2D6}$) and CYP2C19 ($CL_{int, CYP2C19}$) were calculated using Simcyp retrograde calculator based on the estimated $f_{m,2D6}$ and systemic atomoxetine clearance measured after intravenous administration to CYP2D6 EM subjects (CDER, 2002). Based on this approach the $CL_{int,CYP2D6}$ was 25.4 µL/min/pmol and the $CL_{int,CYP2C19}$ was 1.84 µL/min/pmol, respectively. Renal clearance was calculated by dividing the total amount of atomoxetine excreted in urine up to infinity by atomoxetine AUC in CYP2D6 EM subjects following administration of radiolabeled atomoxetine to healthy subjects (Sauer *et al.*, 2003). Inhibition constants of atomoxetine for CYP2D6 and CYP3A4 were collected from the literature (Sauer *et al.*, 2004). All the pharmacokinetic parameters used for model development are summarized in Table 1 and the final atomoxetine drug model is included as supplemental data file.

Atomoxetine volume of distribution was predicted using a full-PBPK model in Simcyp. Out of the two methods available, "method 2" described originally by Rodgers and Rowland (Rodgers and Rowland, 2006) was selected for prediction of tissue to plasma partition coefficients (K_p values) for individual tissues. The predicted V_{ss} value was 0.74 L/kg, compared to the observed atomoxetine V_{ss} of 1.02-1.09 L/kg (CDER, 2002) following iv dosing in healthy subjects.

Simulation of atomoxetine disposition and validation of atomoxetine PBPK model. All simulations were performed using Simcyp population based simulator and a full PBPK model. Virtual Simcyp library populations of healthy volunteers, pediatric population and organ impairment patients were used. For each simulation, a random seed subject selection was implemented except for DDIs where simulations were conducted as fixed seed to account for the crossover trials. For each simulation, a trial of 100 virtual subjects was used with gender and age range of the virtual population matched with reported clinical study data (Supplemental Table 1). If not reported, gender distribution was set as 1:1, and age range 18-55. In addition, all simulations only included Caucasian subjects except the specific simulations for other ethnicities, as majority of subjects in all studies were Caucasians (Supplemental Table 1), and limited mixed population models are available. Seven PK studies (a training set) listed in Table 2 were used for CYP2D6 f_m calculation and model development. After the model was developed, it was validated using 14 trials that included both CYP2D6 EM and PM populations, single and multiple dosing regimens, and FDA approved and off-label dosing regimens that were not used in model development.

Simulation of atomoxetine PK in different ethnic groups. To evaluate the applicability of the validated atomoxetine model to PK prediction in different ethnic groups, atomoxetine disposition was simulated in Chinese and Japanese populations using the Simcyp library Chinese, Japanese, and Caucasian populations with and without an adjustment for atomoxetine intrinsic clearance

based on the activity of CYP2D6*10/*10, a genotype common in Asian population. First, the Simcyp library Chinese and Japanese population models were directly applied to the validated atomoxetine substrate model. For each population, the phenotype was set as either CYP2D6 EM or IM to simulate the CYP2D6 EM and CYP2D6*10/*10 genotyped population, respectively. Second, the Simcyp library Caucasian population model was used to simulate the Asian population studies to examine the appropriateness of different CYP enzyme levels in different population models. Third, a reduced atomoxetine intrinsic clearance was incorporated in the drug file based on in vitro data of atomoxetine intrinsic clearance by CYP2D6*10 enzyme being only 8.6% of the intrinsic clearance by CYP2D6*1 enzyme (Shen *et al.*, 2007). To predict the intrinsic clearance of atomoxetine in CYP2D6*10/*10 genotyped population, the existing pharmacokinetic data in CYP2D6 EM phenotype population with mixed genotypes was analyzed based on the CYP2D6 activity score system (Gaedigk *et al.*, 2008) and the known allele frequencies for CYP2D6 genotypes in different populations (Gaedigk *et al.*, 2017). CYP2D6 activity scores were assigned as described for CYP2D6 alleles and their corresponding activity scores (Gaedigk *et al.*, 2008). For example, CYP2D6*3 and CYP2D6*4 were assigned activity score 0, CYP2D6*9 and CYP2D6*10 were assigned activity score 0.5, and CYP2D6*1 and CYP2D6*2 were assigned activity score 1 and the activity scores for each allele were added to obtain the overall activity score for each subject. Of Caucasian population, 89.3% is phenotypically CYP2D6 EM which includes CYP2D6 activity scores 1, 1.5 and 2 (Gaedigk *et al.*, 2017). The activity score distribution within only CYP2D6 EM Caucasian population is 33.5% for activity score 1, 16.6% for activity score 1.5, and 50% for activity score 2. As a result, the expected mean in vivo atomoxetine clearance in the Caucasian population with this distribution of activity scores is expected to be 79% of that in the population with 100% activity score 2 (calculated based on net EM activity

being 33.5%*1+16.6%*1.5+50%*2 and solving from this the value for activity score 1). Using this calculation the intrinsic clearance in a population with 100% activity score 2 (CYP2D6*1) is 32.0 μL/min/pmol and the intrinsic clearance of atomoxetine in CYP2D6*10/*10 individuals is calculated to be 2.77 μL/min/pmol (0.086*32 μL/min/pmol). This calculated intrinsic clearance in CYP2D6*10/*10 subjects was incorporated into the atomoxetine substrate model when simulating atomoxetine disposition in CYP2D6*10/*10 subjects, and simulations repeated using the Simcyp library Chinese, Japanese, and Caucasian EM population models.

Simulation of atomoxetine PK in DDI studies. To evaluate the applicability of the validated atomoxetine model to predict drug-drug interactions (DDIs), DDI studies that matched those conducted with atomoxetine were simulated. Four DDI studies were identified, providing atomoxetine PK parameters when administered alone or with known CYP2D6 inhibitors (fluoxetine and paroxetine) or probe substrates midazolam (CYP3A) and desipramine (CYP2D6). For these simulations, previously published fluoxetine, paroxetine, and midazolam models (Ke *et al.*, 2013; Sager *et al.*, 2014) and the Simcyp library desipramine model were used. The performance of these models was evaluated using drug specific acceptance criteria calculated using the same method as described for atomoxetine and existing PK data for paroxetine (Calvo *et al.*, 2004; Schoedel *et al.*, 2012), midazolam (Eap *et al.*, 2004; Kharasch *et al.*, 2004), and desipramine (Steiner and Spina, 1987; Spina *et al.*, 1993, 1996, 1997) in healthy subjects. The calculation and the acceptance criteria are summarized in Supplemental Tables 5 and 6. The calculated AUC acceptance criterion fold ranges for paroxetine, midazolam, and desipramine were 0.59-1.69, 0.6-1.66, and 0.54-1.85, respectively. The simulated AUC values of all coadministered drugs were within their acceptance criteria and hence all coadministered drug models were

considered acceptable. Finally, the atomoxetine disposition was simulated in the presence and absence of the coadministered drugs, and the AUC ratios and C_{max} ratios were computed.

Simulation of atomoxetine PK in special populations. To evaluate whether the atomoxetine model validated in healthy adults could be used to predict atomoxetine PK in pediatric population, end stage renal disease (ESRD) patients, and hepatic impairment (HI) patients, atomoxetine disposition in these populations was simulated using the existing Simcyp library special population models. Based on the evaluation of atomoxetine PK variability in these populations, the model performance was assessed using the same criterion as presented for the healthy adult population. For pediatrics simulation, the Simcyp library pediatric population model was used with corresponding CYP2D6 genotype information provided in each study. For hepatic impairment (HI) simulation, the Simcyp Child-Pugh B and Child-Pugh C population models with CYP2D6 EM were used according to the reported trials (CDER, 2002; Chalon *et al.*, 2003). For end stage renal disease (ESRD), the Simcyp eGFR<30 L/hr population was used according to the data in atomoxetine NDA. Since the ESRD clinical study did not specify the CYP2D6 genotypes of the subjects, the CYP2D6 genotype distribution was set as the Simcyp default, i.e. 85% EM, 8% PM and 7% UM in the ESRD population model. In addition, due to the limited number of subjects (N=6) in the ESRD study, 50 trials of 6 subjects were simulated using random seed selection to capture possible inter-study variability due to small sample size and variable genotype distribution. Dialysis data was not available for ESRD population and hence not included in the simulation.

Results

Atomoxetine PBPK model development and validation. The atomoxetine PBPK model (Table 1) was first developed and optimized using a training dataset (See supplemental data for compound

file and representative model output). The training set included both iv and po dosing regimens and CYP2D6 EM and PM populations (Figure 1). All of the simulated AUC and C_{max} values of the training set studies met the pre-defined drug specific model acceptance criteria for AUC and C_{max} (Table 2), confirming model parameters such as absorption rate constant, bioavailability, clearance, and volume of distribution. The model was then validated using a separate test dataset of 14 human PK studies including both CYP2D6 EM and PM populations, single and multiple dosing regimens, and FDA approved and off-label dosing regimens (Table 3). Similar to the training dataset, all of the simulated AUC and C_{max} values for the validation studies were within the acceptance criteria (Table 3). Therefore, the model was considered validated for healthy adult Caucasian subjects with CYP2D6 EM and PM genotypes.

Simulation of atomoxetine PK in different ethnicities. To test whether the atomoxetine model validated in Caucasians could be used to predict atomoxetine disposition in Chinese and Japanese populations, atomoxetine disposition was simulated using the Simcyp built-in Chinese and Japanese population models without any modifications (Table 4). As the reported studies showed PK data separately for CYP2D6 EM and CYP2D6*10/*10 genotyped subjects, atomoxetine disposition was separately simulated using the Chinese and Japanese CYP2D6 EM and IM populations. Overall, using these populations, the majority of the simulated PK parameters did not pass the model acceptance criteria (Table 4): For CYP2D6 EM subjects, only 38% of simulated PK parameters met the study specific acceptance criteria and even these simulations resulted in predictions close to the upper limit of the acceptance range. For CYP2D6*10/*10 genotyped subjects (considered as Japanese and Chinese IM subjects), 63% of simulated PK parameters met the acceptance criteria. Therefore, compared to the 100% simulation success rate in the 14 validation studies, the predictions of atomoxetine disposition in Asian populations using Simcyp

Asian population models was unacceptable. Of note, the Chinese and Japanese population models have presumptively lower CYP2D6 expression than the Caucasian population. This may result in the simulation failure if Caucasian and Asian subjects of similar genotype (same activity score) actually have similar CYP2D6 protein expression levels. To test this, atomoxetine disposition in Japanese and Chinese populations was simulated using the Caucasian population model. Doing so, 100% atomoxetine PK parameters in Chinese and Japanese EM subjects were acceptably predicted. In addition, the atomoxetine specific intrinsic clearance changes in CYP2D6*10/*10 subjects were incorporated into the model based on published in vitro data, to test whether in vitro pharmacogenetic data could be used to reliably predict in vivo disposition in this genotype group. Doing so, the Chinese and Japanese population models poorly predicted atomoxetine PK parameters in Chinese and Japanese CYP2D6*10/*10 subjects with 0% success rate. On the other hand, after applying the intrinsic clearance changes, Caucasian population model predicted the disposition of atomoxetine in Chinese and Japanese CYP2D6*10/*10 subjects with 75% success rate.

Simulation of atomoxetine PK in DDI studies. To evaluate the applicability of the validated model in predicting atomoxetine disposition in DDI scenarios, atomoxetine disposition was simulated when coadministered with the CYP2D6 inhibitors fluoxetine and paroxetine and the probe drugs desipramine and midazolam (Table 5). The PBPK models for all the coadministered drugs resulted in simulated AUC and C_{max} values within their acceptance criteria (Supplemental Table 7). Overall, for a total of 12 simulated DDI trials, atomoxetine AUC was predicted acceptably in 11 (92%) trials and the C_{max} was predicted acceptably in 8 (67%) trials (Table 5). The only study in which atomoxetine AUC was not predicted within the acceptance criteria was a study in which 40 mg atomoxetine was coadministered with desipramine (Table 5). In the same

study, the AUC value following 60 mg dosing of atomoxetine was accurately predicted. In the observed data, there was no dose-proportional increase in atomoxetine AUC between the 40 mg (n=6) and 60 mg (n=15) dose groups despite atomoxetine having linear kinetics. Based on this discrepancy in the experimental data, possibly due to the small sample size (N=6) in the 40 mg dose group, the 92% performance rate of the model was considered acceptable.

The effect of CYP2D6 inhibition by paroxetine on atomoxetine AUC and C_{max} was well predicted. In the two paroxetine DDI studies, 100% of atomoxetine AUC and C_{max} values met the acceptance criteria (Table 6). Furthermore, atomoxetine AUC was reported to increase 7.0-fold (CDER, 2002) and 5.6-fold (Todor *et al.*, 2015), respectively, and the corresponding predicted increases were 6.7-fold and 5.9-fold. Similarly, atomoxetine C_{max} was reported to increase 3.8-fold (CDER, 2002) and 1.7-fold (Todor *et al.*, 2015) while a 3.9- and 1.5-fold increase in C_{max} was predicted in the two studies, respectively. For the paroxetine DDI study with available plasma-concentration time data points, all the observed data points were within the 95% confidence interval of the simulations (Figure 2). These results demonstrate an excellent agreement between the observed and simulated DDIs. However, in the presence of fluoxetine, the atomoxetine C_{max} values were under-predicted despite the AUC values being within the acceptance criteria. As the plasma concentration-time curves for this study were not available, the quality of the experimental data for C_{max} determination could not be assessed. The fold change in atomoxetine AUC in the presence of fluoxetine could not be evaluated as the data from the control session in this study was not available. Moreover, as expected, there was no change in atomoxetine AUC or C_{max} after co-administration of midazolam or desipramine (both administered as a single dose) with atomoxetine (Table 5). Importantly, the PBPK modeling also accurately predicted midazolam and desipramine disposition in the presence

and absence of coadministered atomoxetine and the lack of a DDI in these scenarios (Supplemental Table 7).

Simulation of atomoxetine PK in special populations. To evaluate the applicability of the validated model in predicting atomoxetine disposition in special populations, atomoxetine disposition was simulated in pediatric subjects, ESRD and HI patients. When atomoxetine disposition was simulated in pediatric population, all simulated AUC and C_{max} values for the 4 trials were within the acceptance criteria (Table 6). Based on this data, the validated model could be successfully applied to predict atomoxetine disposition in both EM and PM pediatric population. The observed plasma concentration-time curves for the pediatric trials were all within the 95% confidence interval of the predicted mean (Figure 3).

The predicted atomoxetine AUC in ESRD was 2-fold greater than that in the matching healthy population (Table 6). This magnitude of increase in atomoxetine AUC (ratio of AUC in ESRD over healthy) is in agreement with the reported data of the AUC change in ESRD (CDER, 2002)(Table 6). However, neither the overall simulated AUC nor the C_{max} met the acceptance criteria in either healthy subjects or in the ESRD patients. This could potentially be due to the small sample size (n=6) of the ESRD study and the variability of the data in this population. When the 50 simulated trials of ESRD patients were assessed, only 20% of these met the acceptance criteria of AUC (Figure 4) and none of them met the acceptance criteria of C_{max}. It is also noteworthy that the observed AUC in the healthy subject group in the ESRD study would not have met the acceptance criteria for atomoxetine AUC in the healthy subject studies with the same dosage (20 mg) and this AUC is not within the observed AUCs in healthy population.

When atomoxetine disposition was simulated in the population with moderate and severe HI in comparison to healthy controls, a 4 to 10-fold increase in atomoxetine AUC was predicted in HI

compared to the control (Table 6). This predicted effect of HI greatly exceeded the observed 1 to 2.5-fold increase in atomoxetine AUC in HI. While the model predicted atomoxetine disposition in healthy subjects within the acceptance criteria, both of the AUC and C_{max} were significantly overpredicted in the HI populations and these simulations did not meet the model acceptance criteria.

Discussion

The goal of this study was to evaluate whether a drug PBPK model validated against a comprehensive in vivo PK dataset in healthy volunteers with different genotypes, could be used with previously developed population models to simulate drug disposition in specific patient groups. Atomoxetine, a well characterized CYP2D6 probe was used as the model drug. A full PBPK model was developed and validated for atomoxetine, and this model can be used in the future to simulate atomoxetine disposition in healthy volunteers. This study is the first of its kind to cross-evaluate population models for a probe drug with a validated drug model. Overall, the findings are consistent with previous reports emphasizing low confidence in population models for HI, ESRD and different ethnicities, but confirm high confidence in PBPK modeling in healthy volunteers and in DDI studies (Jones *et al.*, 2015, Wagner *et al.*, 2015). Importantly, due to the rigorous model development-validation-extrapolation workflow employed, the findings of this study allow differentiating potential causes of low confidence in specific population simulations including questions of clinical data quality and uncertainties in population models.

It has been suggested that small clinical studies and high intrinsic variability in PK contribute to poor model performance (Abduljalil *et al.*, 2014). To address this issue, this study used a statistical

model acceptance criterion (Abduljalil *et al.*, 2014) that is calculated specifically for the drug of interest based on the observed PK variability of that drug. This criterion is based on the 99.998% CI of all observed clinical data, and hence it is expected that nearly all simulations will be within this criterion regardless of the study size or data variability, as only 0.002% of clinical data should be outside of the criterion range. For atomoxetine, due to the relatively low variability in its disposition, the calculated 99.998% CI was more stringent than the commonly used 2-fold criterion. The acceptance range was 0.56-1.77 fold for EM population and 0.74-1.35 fold for PM population. This is in agreement with previous studies stating that the 2-fold criterion may be scientifically too lenient to assess model quality for some drugs (Abduljalil *et al.*, 2014). The statistical criterion for model evaluation also shows that due to the variability in atomoxetine AUC in the healthy population, the model is not expected to simulate atomoxetine AUC within a criterion analogous to bioequivalence (1.25-fold (Guest *et al.*, 2011)) in 9.7% of healthy volunteer studies in EMs (calculated based on critical value of 1.658 for 1.25-fold error from equations 1-3). Indeed, 25% of AUC values of the verification and validation studies in healthy volunteers with EM phenotype were not simulated within the 1.25-fold criterion (Supplemental table 8). In contrast, as predicted from the lower variability in PM populations, atomoxetine AUC was predicted within 1.25-fold in all CYP2D6 PM studies. Taken together, this analysis shows that the commonly used goal of "fit-for-purpose" for PBPK model performance should be considered in the context of the intrinsic variability of the drug of interest. Essentially, the criterion used here can be applied to establish confidence on what fraction of clinical trials are expected to be predicted within the "fit-for-purpose" n-fold criteria and to determine how many clinical studies should be analyzed to establish confidence in the drug model.

The data shown here clearly identifies population models as the primary reason for poor PBPK model extrapolation regardless of model acceptance criteria used. The role of population models in contributing to poor simulation performance is clearly shown in the simulation of Asian populations using the population models for Caucasians, Japanese and Chinese. Atomoxetine disposition in Japanese and Chinese EM subjects was best predicted using Caucasian EM population model instead of Chinese or Japanese population models. CYP2D6*10 allele has been shown to be much more prevalent in Asian populations than in Caucasians (Kitada, 2003) resulting in apparent lower population CYP2D6 activity. In agreement with this phenotype, the Chinese and Japanese population models in Simcyp have lower CYP2D6 expression levels (4 and 4.5 pmol/mg) than the Caucasian population (8 pmol/mg). The low CYP2D6 expression levels in the Asian population models explain the simulation failures observed with Japanese and Chinese population studies, and the data obtained here strongly suggests CYP2D6 protein expression levels are similar between Asian and Caucasian populations. If the populations are genotyped for CYP2D6, the Caucasian population model is superior to the Asian population models. As atomoxetine is a well characterized CYP2D6 probe, it is likely that these results can be extrapolated to other CYP2D6 substrates as well. The fact that the Caucasian model with an intrinsic clearance adjusted based on CYP2D6*10/*10 genotype overpredicted 25% of the observed atomoxetine PK parameters (AUC and C_{max}) may be due to poor extrapolation of in vitro enzyme activity to in vivo. This interpretation is supported by the fact that while in vitro CYP2D6*10 had only 8% of the activity of CYP2D6*1 (Shen *et al.*, 2007), the in vivo activity score of CYP2D6*10 is 0.5 (Gaedigk *et al.*, 2008) suggesting only 50% difference in the in vivo activity between CYP2D6*10 and CYP2D6*1.

The results of this study support the consensus that PBPK models can be used to predict drug disposition in pediatric populations above 2 years of age (Jones *et al.*, 2015, Wagner *et al.*, 2015). The model accurately predicted atomoxetine disposition in pediatric populations with defined genotypes suggesting that the disposition of CYP2D6 substrates can be extrapolated using full PBPK models from adult studies to pediatrics even in different genotype groups. In contrast, the validated atomoxetine model could not reliably predict atomoxetine disposition in ESRD or in HI using the existing RI and HI population models. It is highly unlikely that this failure is due to the small sample size (6, 6, and 4 in the ESRD trial, Child-Pugh B trial, and Child-Pugh C trial, respectively) or high variability of atomoxetine disposition in these studies. The AUC acceptance criteria calculated based on the observed variability and sample size in the organ impairment studies is 0.34-2.92-fold for ESRD trial, 0.54-1.86-fold for Child-Pugh B and 0.29-3.43-fold for Child-Pugh C and the simulated AUC values do not meet these acceptance criteria. Similarly, all of these simulations also failed when using the common 2-fold criterion (Supplemental table 8). Atomoxetine is almost entirely cleared via hepatic metabolism and as such the population model parameters that result in the simulated 2-fold increase in atomoxetine AUC in the ESRD population are not clear. The current label of atomoxetine states that renal impairment does not affect atomoxetine disposition, presumably because the body weight normalized clearance of atomoxetine was not different in ESRD patients and controls despite the 2-fold change in the AUC of atomoxetine. This lack of change in clearance of atomoxetine in ESRD group was not captured here suggesting that the confidence in the ESRD population model for at least CYP2D6 substrates is low. The poor performance of the ESRD model was unexpected as previous studies have successfully (within 1.5-fold) simulated bisoprolol disposition in RI population using full PBPK model (Li *et al.*, 2012) and orteronel disposition in RI population using minimal PBPK model (Lu

et al., 2014) although no comprehensive model validation across healthy volunteers and different special populations was presented. As both of these drugs are mainly renally cleared, it is possible that the simulation failure here is specific to metabolically cleared drugs. In addition, differences between the full PBPK model population and minimal PBPK model population may contribute to the simulation failure, and further studies with broader range of drugs are needed to evaluate these possibilities. It is known that renal impairment can affect the activity of drug metabolizing enzymes in the liver and the clearance and distribution characteristics of mainly metabolically cleared drugs (Zhao *et al*., 2012; Touchette MA and Slaughter RL 1991). It has also been suggested that renal impairment affects CYP2D6 cleared drugs more than some of the other CYP enzymes (Zhao *et al*., 2012; Touchette MA and Slaughter RL 1991). The results here suggest that this hepatorenal coupling in renal disease is not sufficiently well characterized to allow reliable simulations of CYP2D6 substrates in RI and the effect of RI on hepatic clearance may be overestimated.

For the HI studies, the overprediction in AUC is likely because of an overestimation in the magnitude of decrease in CYP2D6 expression and liver size in the Simcyp HI population model. In the Simcyp library Child-Pugh B and Child-Pugh C population models, CYP2D6 expression is decreased by 67.5% and 89.5%, and the liver volume is similarly decreased by 29% and 39.4%, respectively. The data collected here suggests that this is an overestimation of the decrease in CYP2D6 expression/activity in the HI population. Using the validated atomoxetine model, the decrease in CYP2D6 expression in the HI population can be estimated based on the observed 1.7- to 3.7-fold increase in atomoxetine AUC in moderate and severe HI. If the change in liver volume is kept as defined in the HI population model, no change in CYP2D6 expression in moderate HI patients, and a decrease of 25% in CYP2D6 expression in severe HI patients is estimated. In

contrast, if there is no change in liver volume, the CYP2D6 expression level is predicted to decrease 32% and 89% in moderate and severe HI patients. A larger number of CYP2D6 substrates need to be studied via rigorous simulation approaches to determine whether this predicted % change in CYP2D6 expression is correct in HI. In addition, further studies with CYP2D6 substrates with different plasma protein binding and different effects of HI on plasma protein binding need to be evaluated to delineate altered plasma protein binding in HI from altered CYP activity in contributing to simulation accuracy. However, taken together, this data demonstrates a lack of adequate knowledge and confidence in the physiological changes and enzyme expression in the organ impairment populations to allow PBPK based predictions.

Authorship Contributions

Participated in research design: Huang, Ragueneau-Majlessi, Isoherranen

Conducted experiments: Huang, Nakano, Sager

Performed data analysis: Huang, Isoherranen.

Wrote or contributed to the writing of the manuscript: Huang, Nakano, Sager, Ragueneau-Majlessi, Isoherranen

References

Abduljalil K, Cain T, Humphries H, and Rostami-Hodjegan A (2014) Deciding on success criteria for predictability of pharmacokinetic parameters from in vitro studies: An analysis based on in vivo observations. *Drug Metab Dispos* **42**:1478–1484.

Belle DJ, Ernest CS, Sauer J-M, Smith BP, Thomasson HR, and Witcher JW (2002) Effect of potent CYP2D6 inhibition by paroxetine on atomoxetine pharmacokinetics. *J Clin Pharmacol* **42**:1219–27.

Brown JT, Abdel-Rahman SM, van Haandel L, Gaedigk A, Lin YS, and Leeder JS (2016) Single dose, CYP2D6 genotype-stratified pharmacokinetic study of atomoxetine in children with ADHD. *Clin Pharmacol Ther* **0**:1–9.

Calvo G, García-Gea C, Luque A, Morte A, Dal-Ré R, and Barbanoj M (2004) Lack of pharmacologic interaction between paroxetine and alprazolam at steady state in healthy volunteers. *J Clin Psychopharmacol* **24**:268–276.

CDER (2002) Application number 21-411. Clinical Pharmacology and biopharmaceutics review(s).

CDER (2012) Guidance for industry: Drug interaction studies–study design, data analysis, implications for dosing, and labeling recommendations. U.S. Food and Drug Administration, Silver Spring, MD.

Chalon SA, Desager JP, DeSante KA, Frye RF, Witcher J, Long AJ, Sauer JM, Golnez JL, Smith BP, Thomasson HR, and Horsmans Y (2003) Effect of hepatic impairment on the pharmacokinetics of atomoxetine and its metabolites. *Clin Pharmacol Ther* **73**:178–191.

CHMP (2005) Guideline on the Evaluation of the pharmacokinetics of medicinal products in patients with impaired hepatic function. CPMP/EWP/2339/02, European Medicines Agency, London.

Choi C-I, Bae J-W, Lee Y-J, Lee H-I, Jang C-G, and Lee S-Y (2014) Effects of CYP2C19 genetic polymorphisms on atomoxetine pharmacokinetics. *J Clin Psychopharmacol* **34**:139–142.

Cui YM, Teng CH, Pan AX, Yuen E, Yeo KP, Zhou Y, Zhao X, Long AJ, Bangs ME, and Wise SD (2007) Atomoxetine pharmacokinetics in healthy Chinese subjects and effect of the CYP2D6*10 allele. *Br J Clin Pharmacol* **64**:445–449.

Eap CB, Buclin T, Cucchia G, Zullino D, Hustert E, Bleiber G, Golay KP, Aubert A-C, Baumann P, Telenti A, and Kerb R (2004) Oral administration of a low dose of midazolam (75 microg) as an in vivo probe for CYP3A activity. *Eur J Clin Pharmacol* **60**:237–246.

Edginton AN, Schmitt W, and Willmann S (2006) Development and Evaluation of a Generic Physiologically Based Pharmacokinetic Model for Children. *Clin Pharmacokinet* **45**:1013–1034.

Edginton AN, and Willmann S (2008) Physiology-based simulations of a pathological condition: Prediction of pharmacokinetics in patients with liver cirrhosis. *Clin Pharmacokinet* **47**:743–752.

Gaedigk A, Sangkuhl K, Whirl-Carrillo M, Klein T, and Leeder JS (2017) Prediction of CYP2D6 phenotype from genotype across world populations. *Genet Med* **19**:69–76.

Gaedigk A, Simon SD, Pearce RE, Bradford LD, Kennedy MJ, and Leeder JS (2008) The

CYP2D6 activity score: translating genotype information into a qualitative measure of phenotype. *Clin Pharmacol Ther* **83**:234–42.

Guest EJ, Aarons L, Houston JB, Rostami-Hodjegan A, and Galetin A (2011) Critique of the two-fold measure of prediction success for ratios: Application for the assessment of drug-drug interactions. *Drug Metab Dispos* **39**:170–173.

Huang SM, Abernethy DR, Wang Y, Zhao P, and Zineh I (2013) The utility of modeling and simulation in drug development and regulatory review. *J Pharm Sci* **102**:2912–2923.

Huang SM, and Rowland M (2012) The Role of Physiologically Based Pharmacokinetic Modeling in Regulatory Review. *Clin Pharmacol Ther* **91**:542–549.

Ito K, Hallifax D, Obach RS, Houston JB. (2005) Impact of parallel pathways of drug elimination and multiple cytochrome P450 involvement on drug-drug interactions: CYP2D6 paradigm. *Drug Metab Dispos.* **33**:837-44.

Jamei M, Marciniak S, Feng K, Barnett A, Tucker GT, and Rostami-Hodjegan A (2009) The Simcyp ® Population-based ADME Simulator. *Expert Opin Drug Metab Toxicol* **5**:211–223.

Johnson TN, Boussery K, Rowland-Yeo K, Tucker GT, and Rostami-Hodjegan A (2010) A semi-mechanistic model to predict the effects of liver cirrhosis on drug clearance. *Clin Pharmacokinet* **49**:189–206.

Johnson TN, Rostami-Hodjegan A, and Tucker GT (2006) Prediction of the Clearance of Eleven Drugs and Associated Variability in Neonates, Infants and Children. *Clin Pharmacokinet* **45**:931–956.

Jones HM, Chen Y, Gibson C, Heimbach T, Parrott N, Peters SA, Snoeys J, Upreti V V, Zheng M, and Hall SD (2015) Physiologically based pharmacokinetic modeling in drug discovery and development: a pharmaceutical industry perspective. *Clin Pharmacol Ther* **97**:247–262.

Jones HM, Gardner IB, and Watson KJ (2009) Modelling and PBPK simulation in drug discovery. *AAPS J* **11**:155–66.

Ke AB, Nallani SC, Zhao P, Rostami-Hodjegan A, Isoherranen N, and Unadkat JD (2013) A physiologically based pharmacokinetic model to predict disposition of CYP2D6 and CYP1A2 metabolized drugs in pregnant women. *Drug Metab Dispos* **41**:801–813.

Kharasch ED, Walker A, Hoffer C, and Sheffels P (2004) Intravenous and oral alfentanil as in vivo probes for hepatic and first-pass cytochrome P450 3A activity: Noninvasive assessment by use of pupillary miosis. *Clin Pharmacol Ther* **76**:452–466.

Kitada M (2003) Genetic polymorphism of cytochrome P450 enzymes in Asian populations: focus on CYP2D6. *Int J Clin Pharmacol Res* **23**:31–5.

Li G, Wang K, Chen R, Zhao H, Yang J, and Zheng Q (2012) Simulation of the pharmacokinetics of bisoprolol in healthy adults and patients with impaired renal function using whole-body physiologically based pharmacokinetic modeling. *Acta Pharmacol Sin* **33**:1359–71.

Lu C, Suri A, Shyu WC, and Prakash S (2014) Assessment of cytochrome P450-mediated drug-drug interaction potential of orteronel and exposure changes in patients with renal impairment using physiologically based pharmacokinetic modeling and simulation. *Biopharm Drug Dispos* **35**:543–552.

Matsui A, Azuma J, Witcher JW, Long AJ, Sauer J-M, Smith BP, DeSante KA, Read HA., Takahashi M, and Nakano M (2012) Pharmacokinetics, Safety, and Tolerability of Atomoxetine and Effect of CYP2D6*10/*10 Genotype in Healthy Japanese Men. *J Clin Pharmacol* **52**:388–403.

Ring BJ, Gillespie JS, Eckstein JA, Wrighton SA (2002) Identification of the human cytochromes P450 responsible for atomoxetine metabolism. *Drug Metab Dispos* **30**:319–323.

Rodgers T, and Rowland M (2006) Physiologically based pharmacokinetic modelling 2: Predicting the tissue distribution of acids, very weak bases, neutrals and zwitterions. *J Pharm Sci* **95**:1238–1257.

Rowland M, Peck C, and Tucker G (2011) Physiologically-based pharmacokinetics in drug development and regulatory science. *Annu Rev Pharmacol Toxicol* **51**:45–73.

Rowland Yeo K, Aarabi M, Jamei M, and Rostami-Hodjegan a (2011) Modeling and predicting drug pharmacokinetics in patients with renal impairment. *Expert Rev Clin Pharmacol* **4**:261–274.

Sager JE, Lutz JD, Foti RS, Davis C, Kunze KL, and Isoherranen N (2014) Fluoxetine- and norfluoxetine-mediated complex drug-drug interactions: in vitro to in vivo correlation of effects on CYP2D6, CYP2C19, and CYP3A4. *Clin Pharmacol Ther* **95**:653–62.

Sauer J-M, Long AJ, Ring B, Gillespie JS, Sanburn NP, DeSante K a, Petullo D, VandenBranden MR, Jensen CB, Wrighton S a, Smith BP, Read H a, and Witcher JW (2004) Atomoxetine hydrochloride: clinical drug-drug interaction prediction and outcome. *J Pharmacol Exp Ther* **308**:410–418.

Sauer JM, Ponsler GD, Mattiuz EL, Long AJ, Witcher JW, Thomasson HR, and Desante KA (2003) Disposition and metabolic fate of atomoxetine hydrochloride: The role of CYP2D6 in human disposition and metabolism. *Drug Metab Dispos* **31**:98–107.

Schoedel KA, Pope LE, and Sellers EM (2012) Randomized open-label drug-drug interaction trial of dextromethorphanquinidine and paroxetine in healthy volunteers. *Clin Drug Investig* **32**:157–169.

Shen H, He MM, Liu H, Wrighton SA, Wang L, Guo B, and Li C (2007) Comparative metabolic capabilities and inhibitory profiles of CYP2D6.1, CYP2D6.10, and CYP2D6.17. *Drug Metab Dispos* **35**:1292–1300.

Spina E, Avenoso A, Campo GM, Caputi AP, and Perucca E (1996) Phenobarbital induces the 2-hydroxylation of desipramine. *Ther Drug Monit* **18**:60–64.

Spina E, Avenoso A, Campo GM, Scordo MG, Caputi AP, and Perucca E (1997) Effect of ketoconazole on the pharmacokinetics of imipramine and desipramine in healthy subjects. *Br J Clin Pharmacol* **43**:315–8.

Spina E, Pollicino AM, Avenoso A, Campo GM, Perucca E, and Caputi AP (1993) Effect of fluvoxamine on the pharmacokinetics of imipramine and desipramine in healthy subjects. *Ther Drug Monit* **15**:243–6.

Steiner E, and Spina E (1987) Differences in the inhibitory effect of cimetidine on desipramine metabolism between rapid and slow debrisoquin hydroxylators. *Clin Pharmacol Ther* **42**:278–82.

Todor I, Popa A, Neag M, Muntean D, Bocsan C, Buzoianu A, Vlase L, Gheldiu A, Chira R, and

Briciu C (2015) The Influence of Paroxetine on the Pharmacokinetics of Atomoxetine and Its Main Metabolite. *Clujul Med* **88**:513.

Touchette MA and Slaughter RL. (1991) The effect of renal failure on hepatic drug clearance. *DICP: the annals of pharmacotherapy* **25**:1214-1224

Wagner C, Zhao P, Pan Y, Hsu V, Grillo J, Huang SM, and Sinha V (2015) Application of Physiologically Based Pharmacokinetic (PBPK) Modeling to Support Dose Selection: Report of an FDA Public Workshop on PBPK. *CPT pharmacometrics Syst Pharmacol* **4**:226–30.

Yang J, Jamei M, Yeo KR, Tucker GT, and Rostami-Hodjegan A (2007) Prediction of intestinal first-pass drug metabolism. *Curr Drug Metab* **8**:676–684.

Zhao P, Rowland M, Huang SM. (2012) Best practice in the use of physiologically based pharmacokinetic modeling and simulation to address clinical pharmacology regulatory questions. *Clin Pharmacol Ther.* **92**:17-20.

Footnotes

This study was supported in part by a grant from the National Institutes of Health (NIH) [P01DA032507] by the Research Participation Program at the Center for Drug Evaluation and Research administered by the Oak Ridge Institute for Science and Education (ORISE) through an interagency agreement between the U.S. Department of Energy and the U.S. Food and Drug Administration (FDA).

Figure legends

Figure 1. The workflow of developing and validating atomoxetine full-PBPK model and extrapolating the validated model to predict atomoxetine disposition in different ethnicities, special populations, and DDIs.

Figure 2. Simulated and observed plasma concentration time curves for atomoxetine in the presence of placebo (a) and paroxetine (b). The red dots indicate the observed data with its standard deviation, the black line shows the mean of the simulated data and the blue dashed lines show the 95% confidence intervals of the simulated data.

Figure 3. Simulated and observed plasma concentration time curves for atomoxetine for the pediatric trials reported in the literature. Panel (a) shows the simulation of the plasma-concentration time curve from the publicly available NDA file. Panels b-d show the plasma-concentration time curves in genotyped pediatric subjects with an activity score of 1 (b) activity score of 2 (c) or a PM genotype (d) as reported for observed data in (Brown *et al.*, 2016). The red dots indicate the observed data with its standard deviation, the black line shows the mean of the simulated data and the blue dashed lines show the 95% confidence intervals of the simulated data.

Figure 4. Simulated AUC and C_{max} values for the 50 individual trials in the healthy patients (a and b) and in ESRD patients (c and d) in comparison to the observed study data and its standard deviation. None of the subjects in this study were genotyped.

DMD Fast Forward. Published on August 31, 2017 as DOI: 10.1124/dmd.117.076455
This article has not been copyedited and formatted. The final version may differ from this version.

Table 1. Physicochemical and pharmacokinetic parameters of atomoxetine used in the PBPK model development

Parameter	Value	References
Physicochemical		
Molecular Weight (g/mol)	255.36	Stattera NDA
LogP	3.9	NDA
pKa	9.8	NDA
f_u	0.025	NDA
B/P	0.623	Simcyp prediction toolbox
Absorption		
F_a	0.96	
k_a (L/h)	1.2	optimized
Q_{gut} (L/h)	11.9	Simcyp prediction toolbox
Distribution		
V_{ss} (L/kg)	0.74	Simcyp prediction full PBPK method 2
Metabolism/elimination		
$CL_{i.v.}$ (L/hr)	16.3	NDA
CL_r (L/hr)	0.185	Sauer et al. (Sauer *et al.*, 2003)
$f_{m,CYP2D6}$	0.876	
Recombinant CL_{int} (µL/min/pmol)		
CYP2D6	25.4	
CYP2C19	1.84	
CYP enzyme abundance (pmol/mg microsomal protein)		
CYP2D6 EM	8 (61)[a]	Simcyp default value
CYP2C19 EM	14 (40)[a]	optimized
Interaction		
CYP2D6 K_i (µM)	34.3	(Sauer *et al.*, 2004)
CYP3A4 K_i (µM)	3.6	(Sauer *et al.*, 2004)

B/P blood to plasma ratio, *CLi.v.* clearance after intravenous administration, *CLr* renal clearance, *CYP* cytochrome P450, F_a fraction absorbed, f_m fraction metabolism, *fu* fraction unbound in plasma, k_a absorption rate constant, K_i inhibition constant, *LogP* log octanol:water partition coefficient, Q_{gut} drug absorption flow to intestine

[a.] Mean value (Coefficient of Variance)

DMD Fast Forward. Published on August 31, 2017 as DOI: 10.1124/dmd.117.076455
This article has not been copyedited and formatted. The final version may differ from this version.

Table 2. Model development PK dataset. The clinical studies used as the training set and the simulated and observed AUC and C_{max} values for these studies are shown for the EM and PM populations and for the oral (po) and intravenous (iv) route of administration. All trial names are from the NDA file (CDER, 2002).

Trial	Dose (mg)	Mean observed AUC (μg.hr/ml)	AUC acceptance range (μg.hr/ml)	Mean simulated AUC (μg.hr/ml)	Mean observed C_{max} (ng/ml)	C_{max} acceptance range (ng/ml)	Mean simulated C_{max} (ng/ml)
EM population po dosing							
B4L-LC-HFBJ	10[a]	0.51	0.30-0.88	0.49	85	64-112	79
B4L-LC-HFBJ	90[a]	5.47	3.17-9.41	4.35	813	618-1073	715
B4Z-LC-LYAE	30[b]	1.22	0.71-2.10	1.44	320	243-422	278
PM population po dosing							
B4L-LC-HFBJ	10[a]	4.21	3.20-5.50	5.21	171	127-231	207
B4L-LC-HFBJ	90[a]	36.7	27.9-48.1	39.7	1518	1123-2049	1237
B4Z-LC-LYAE	30[b]	11.9	9.04-15.6	12.4	1264	935-1706	1087
EM population iv dosing							
B4Z-LC-LYAM	20[a]	1.37	0.77-2.42	1.72	663	504-875	628

[a.] Dosing regimen once every day
[b.] Dosing regimen twice every day

DMD Fast Forward. Published on August 31, 2017 as DOI: 10.1124/dmd.117.076455
This article has not been copyedited and formatted. The final version may differ from this version.

Table 3. Model validation PK dataset. The clinical studies used as the validation set and the simulated and observed mean AUC and C_{max} values for these studies are shown for the EM and PM populations and for the approved and off-label dosing regimens. All trial names are from the NDA file (CDER, 2002).

Trial	Dose (mg)	Mean observed AUC (μg.hr/ml)	AUC acceptance range (μg.hr/ml)	Mean simulated AUC (μg.hr/ml)	Mean observed C_{max} (ng/ml)	C_{max} acceptance range (ng/ml)	Mean simulated C_{max} (ng/ml)
EM population FDA approved dosing regimen							
B4Z-LC-LYAM	40[a]	1.80	1.04-3.10	1.82	326	248-430	341
B4Z-LC-LYAL	40[a]	2.11	1.22-3.63	1.92	333	253-440	318
B4Z-LC-LYAZ	60[a]	3.02	1.75-5.19	2.8	529	402-698	477
B4L-LC-HFBH	20[b]	1.08	0.63-1.86	1.16	160	121-211	200
B4Z-LC-LYAE	45[b]	1.97	1.14-3.39	2.16	490	372-647	416
PM population FDA approved dosing regimen							
B4Z-LC-LYAK	40[a]	14.5	11.0-19.0	15.9	564	417-761	568
B4L-LC-HFBH	20[b]	8.44	6.41-11.1	9.51	915	677-1235	917
B4Z-LC-LYAE	45[b]	18.0	13.7-23.6	18.6	1868	1382-2522	1631
EM population off label dosing regimen							
B4L-LC-HFBJ	120[a]	7.42	4.16-13.1	5.64	1053	800-1390	1000
B4Z-LC-LYAE	60[b]	2.67	1.50-4.73	3.03	646	491-852	593
B4Z-LC-LYAE	75[b]	3.70	2.07-6.55	3.81	821	624-1084	723
PM population off label dosing regimen							
B4L-LC-HFBJ	120[a]	51.6	38.2-69.7	48.9	2233	1675-2992	1829
B4Z-LC-LYAE	60[b]	26.7	19.8-36.0	26.1	2919	2189-3911	2591
B4Z-LC-LYAE	75[b]	37.4	27.7-50.5	33.2	3999	2999-5359	3288

[a.] Dosing regimen once every day
[b.] Dosing regimen twice every day

DMD Fast Forward. Published on August 31, 2017 as DOI: 10.1124/dmd.117.076455
This article has not been copyedited and formatted. The final version may differ from this version.

Table 4. Simulated and observed atomoxetine PK in different ethnic populations
Atomoxetine disposition in Chinese and Japanese subjects was simulated using the different models in Simcyp as described in methods section

CYP2D6 status	Observed values[b] (acceptance range)	Simulated Asian population[b]	Simulated Caucasian population[b]
AUC (µg.hr/ml)			
Chinese study 40mg single dose (Cui *et al.*, 2007)			
EM	2.24 (1.28-3.97)	3.53	1.95
CYP2D6*10/*10 (IM)	4.96 (2.82-8.78)	7.62	
CYP2D6*10/*10 adjusted[a]		**18.2**	8.10
Chinese study 80mg qD for 7 days (Cui *et al.*, 2007)			
EM	4.43 (2.52-7.84)	7.06	3.36
CYP2D6*10/*10 (IM)	9.69 (5.53-17.2)	16.3	
CYP2D6*10/*10 adjusted[a]		**35.8**	16.3
Japanese study 10mg single dose Trial B4Z-LE-LYAN (CDER, 2002)			
EM	0.44 (0.25-0.78)	**0.93**	0.38
CYP2D6*10/*10 (IM)	0.71 (0.41-1.26)	**2.13**	
CYP2D6*10/*10 adjusted[a]		**6.80**	**2.03**
Japanese study 120mg single dose Trial B4Z-LE-LYAN (CDER, 2002)			
EM	5.26 (3.00-9.31)	**11.2**	4.65
CYP2D6*10/*10 (IM)	9.8 (5.59-17.3)	**25.5**	
CYP2D6*10/*10 adjusted[a]		**81.7**	**24.0**
C_{max} (ng/mL)			
Chinese study 40mg single dose (Cui *et al.*, 2007)			
EM	360 (247-472)	**480**	343
CYP2D6*10/*10 (IM)	530 (403-694)	600	
CYP2D6*10/*10 adjusted[a]		**709**	543
Chinese study 80mg qD for 7 days (Cui *et al.*, 2007)			
EM	815 (619-1068)	**1079**	651
CYP2D6*10/*10 (IM)	1199 (911-1571)	1499	
CYP2D6*10/*10 adjusted[a]		**2319**	1379
Japanese study 10mg single dose Trial B4Z-LE-LYAN (CDER, 2002)			
EM	102 (77.2-133)	124	86
CYP2D6*10/*10 (IM)	125 (95.1-164)	160	
CYP2D6*10/*10 adjusted[a]		**181**	136
Japanese study 120mg single dose Trial B4Z-LE-LYAN (CDER, 2002)			
EM	978 (743-1281)	**1490**	860
CYP2D6*10/*10 (IM)	1271 (966-1665)	**1880**	
CYP2D6*10/*10 adjusted[a]		**2178**	1630

[a.] The intrinsic clearance for atomoxetine was adjusted based on in vitro data as discussed in Method [b.] Geometric mean [c.] Bolded values are outside acceptance range

DMD Fast Forward. Published on August 31, 2017 as DOI: 10.1124/dmd.117.076455
This article has not been copyedited and formatted. The final version may differ from this version.

Table 5. Simulated and observed atomoxetine PK in DDI studies. The observed and predicted mean atomoxetine AUC and C_{max} values together with the acceptance criteria for each study are listed. For the DDI studies both study sessions (control and coadministration) were simulated and are reported. ATM, atomoxetine; FLX, fluoxetine; PRX, paroxetine; DES, desipramine; MDZ, midazolam. All studies were conducted in EM populations except ATM+MDZ

Trial	Dose (mg)	Mean observed AUC (µg.hr/ml)	AUC acceptance range (µg.hr/ml)	Mean simulated AUC (µg.hr/ml)	Mean observed C_{max} (ng/ml)	C_{max} acceptance range (ng/ml)	Mean simulated C_{max} (ng/ml)
ATM+FLX[a]	10	2.82	1.64-4.85	2.02	328	249-433	**242**
	45	14.4	8.35-24.8	9.09	1686	1281-2226	**1110**
ATM[a]	20	0.85	0.491-1.46	0.95	184	139-243	165
ATM+PRX[a]	20	5.97	3.46-10.3	6.39	690	524-911	643
ATM[b]	25	1.15	0.65-2.03	1.13	221	168-290	204
ATM+PRX[b]	25	6.45	3.64-11.4	6.64	373	283-489	304
ATM[a]	40	3.18	1.84-5.47	1.94	552	420-729	**351**
	60	2.69	1.56-4.63	2.92	591	449-780	527
ATM+DES[a]	40	3.47	2.01-5.97	**1.94**	557	423-735	**351**
	60	3.01	1.75-5.18	2.92	647	492-854	527
ATM+MDZ[a,c]	60	23.4	17.8-30.7	24.7	2610	1931-3524	2454
	60	24.3	18.5-31.8	27.1	2694	1996-3637	2663

[a.] Data from the atomoxetine NDA submission (CDER, 2002)
[b.] Data from reference (Todor *et al.*, 2015)
[c.] Data from CYP2D6 PM subjects.
[d.] Bolded values are outside acceptance range

DMD Fast Forward. Published on August 31, 2017 as DOI: 10.1124/dmd.117.076455
This article has not been copyedited and formatted. The final version may differ from this version.

Table 6. Simulated and observed atomoxetine PK in special populations The observed and predicted mean atomoxetine AUC and C_{max} values together with the acceptance criteria for each study are listed. The observed and simulated data are shown for genotyped pediatric populations, for patients with end stage renal disease (ESRD) and healthy controls in the same study, and for hepatic impairment patients (Child-Pugh B, CP-B, and Child-Pugh C, CP-C) and controls in the same study. For ESRD and hepatic impairment studies the ratio of the PK values in disease versus healthy was calculated for observed and simulated data and are also reported.

Population	Mean observed AUC (μg.hr/ml)	AUC acceptance range (μg.hr/ml)	Mean simulated AUC (μg.hr/ml)	Mean observed C_{max} (ng/ml)	C_{max} acceptance range (ng/ml)	Mean simulated C_{max} (ng/ml)
Pediatric Population (CDER, 2002; Brown *et al.*, 2016)						
EM[a]	0.65	0.364-1.14	1.07	144	109-189	167
EM 1[b]	0.89	0.505-1.58	1.17	179	136-234	225
EM 2[c]	1.23	0.692-2.17	1.17	255	194-334	225
PM[d]	12.7	9.35-17.1	12.4	638	479-836	500
End Stage Renal Disease Patient Population Trial B4Z-LC-HFBM (CDER, 2002)						
healthy (H)	0.50	0.28-0.88	**1.47**	92.3	70.1-121	**184**
ESRD	1.00	0.57-1.77	**2.98**	105	80.1-138	**230**
ratio of E-H	2.00		2.03	1.14		1.25
Hepatic Impairment Patient Population Trial B4Z-LC-HFBN (CDER, 2002)						
healthy subjects (H)	0.69	0.394-1.22	0.97	0.142	0.081-0.251	0.17
CP-B	1.16	0.661-2.05	**4.63**	0.115	0.066-0.204	**0.32**
CP-C	2.54	1.45-4.50	**10.4**	0.125	0.071-0.221	**0.41**
ratio of CP-B/H	1.68		4.77	0.81		1.88
ratio of CP-C/H	3.67		10.7	0.88		2.41

[a.] Data from atomoxetine NDA submission file with CYP2D6 EM phenotype population (CDER, 2002)
[b.] Data from subjects with CYP2D6 activity score of 1
[c.] Data from subjects with CYP2D6 activity score of 2
[d.] Data from CYP2D6 PM subjects
[b-d.] Data from Brown et al (Brown *et al.*, 2016)
[e.] Bolded values are outside acceptance range

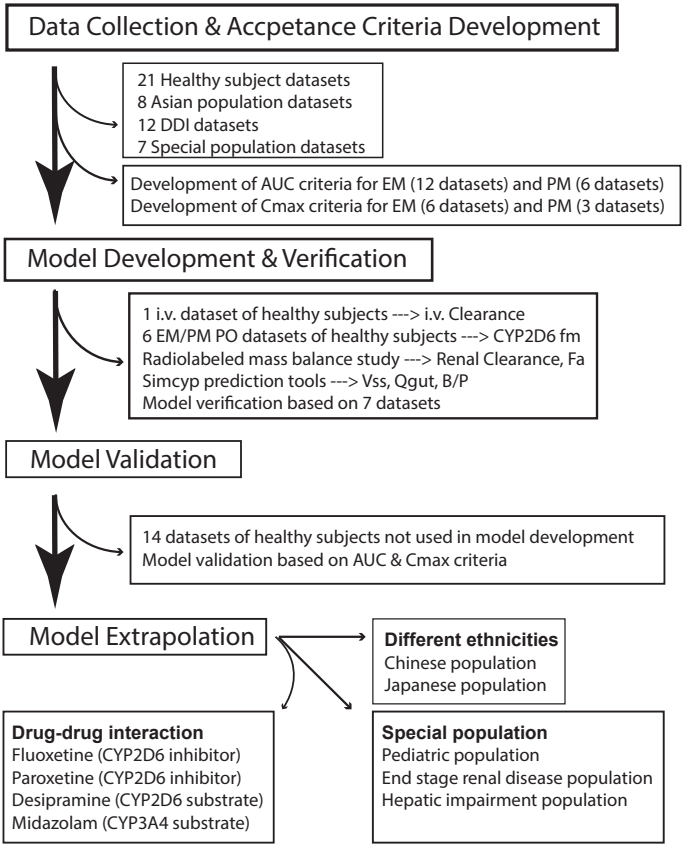
Data Collection & Accpetance Criteria Development
21 Healthy subject datasets
8 Asian population datasets
12 DDI datasets
7 Special population datasets
Development of AUC criteria for EM (12 datasets) and PM (6 datasets)
Development of Cmax criteria for EM (6 datasets) and PM (3 datasets)
Model Development & Verification
1 i.v. dataset of healthy subjects ---> i.v. Clearance
6 EM/PM PO datasets of healthy subjects ---> CYP2D6 fm
Radiolabeled mass balance study ---> Renal Clearance, Fa
Simcyp prediction tools ---> Vss, Qgut, B/P
Model verification based on 7 datasets
Model Validation
14 datasets of healthy subjects not used in model development
Model validation based on AUC & Cmax criteria
Model Extrapolation
Different ethnicities
Chinese population
Japanese population
Drug-drug interaction
Fluoxetine (CYP2D6 inhibitor)
Paroxetine (CYP2D6 inhibitor)
Desipramine (CYP2D6 substrate)
Midazolam (CYP3A4 substrate)
Special population
Pediatric population
End stage renal disease population
Hepatic impairment population

figure1

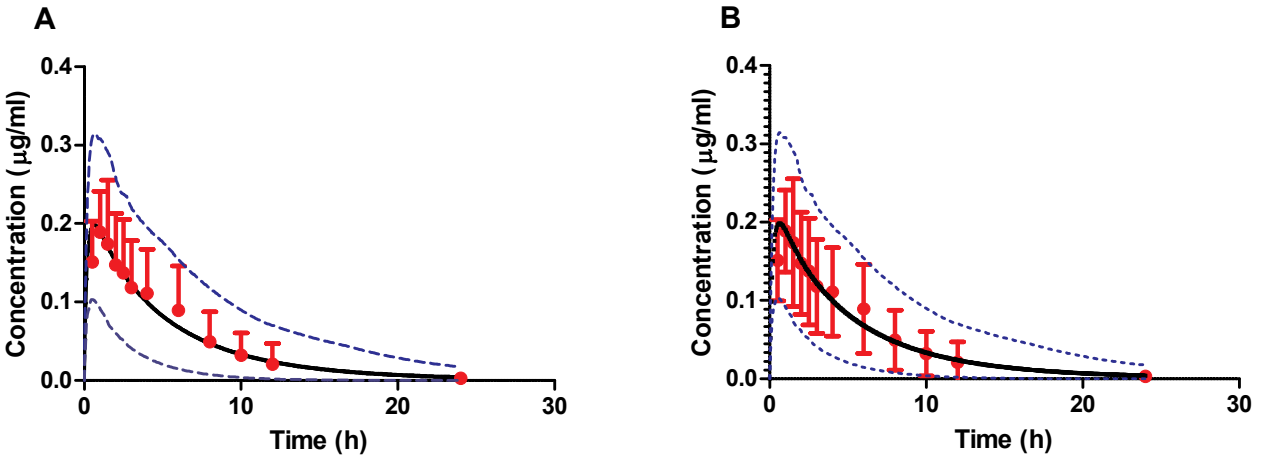

Figure2

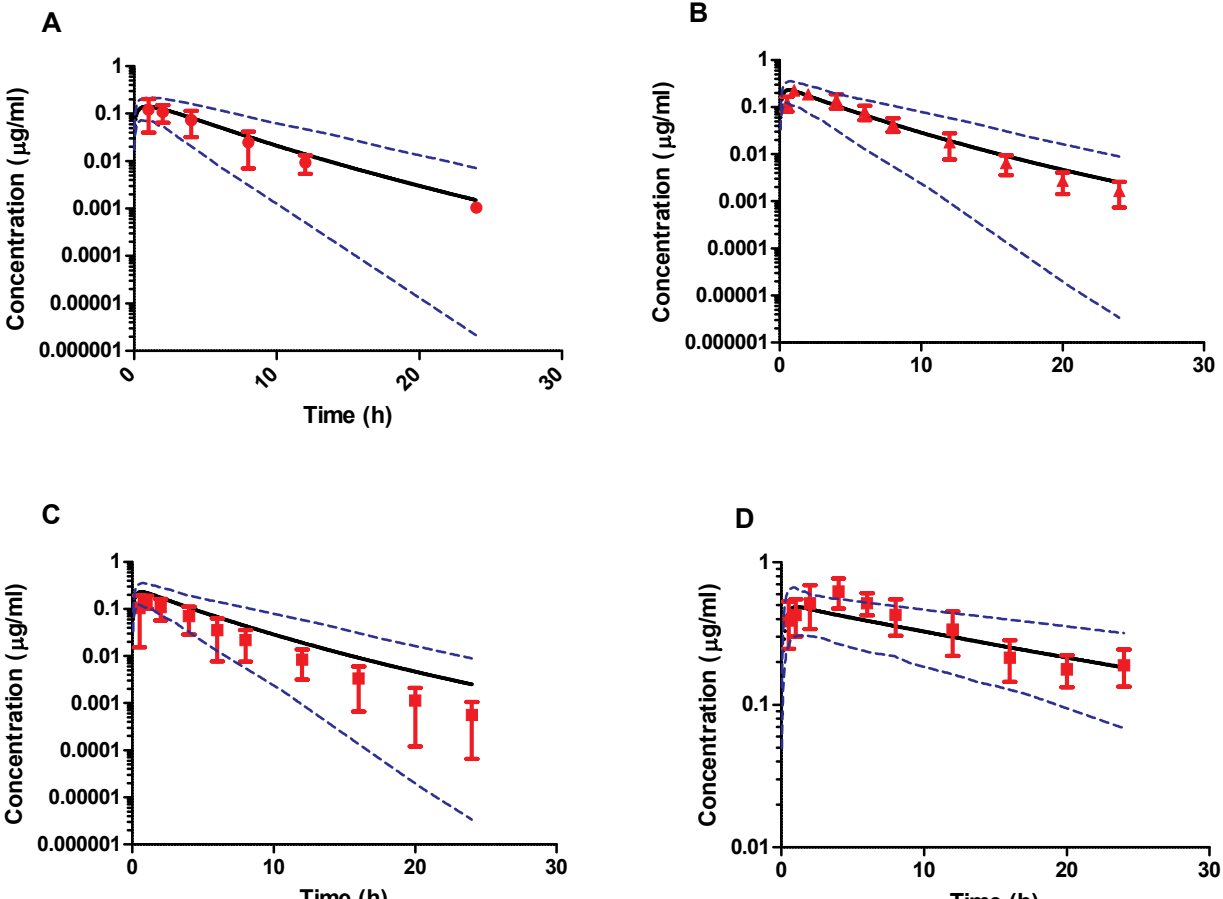
A
B
C
D
Concentration (µg/ml)
Time (h)
1
0.1
0.01
0.001
0.0001
0.00001
0.000001
0
10
20
30

figure3

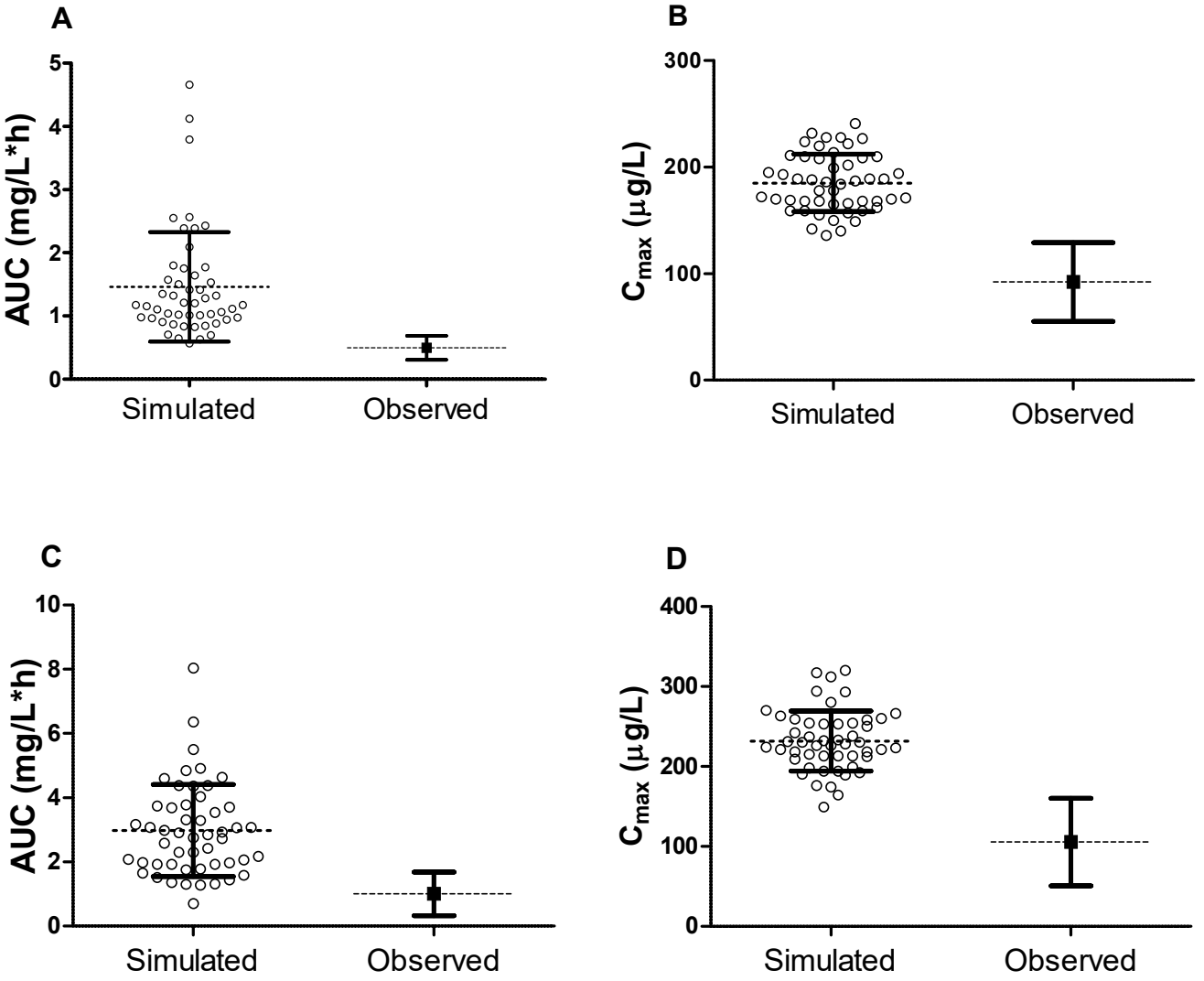
A
AUC (mg/L*h)
0
1
2
3
4
5
Simulated
Observed
B
C_{max} (μg/L)
0
100
200
300
Simulated
Observed
C
AUC (mg/L*h)
0
2
4
6
8
10
Simulated
Observed
D
C_{max} (μg/L)
0
100
200
300
400
Simulated
Observed

figure4